Journal of Systems Engineering and Electronics
Vol. 28, No. 6, December 2017, pp.1174–1185



# Finite-time attitude tracking control for spacecraft without angular velocity measurements

Li Yuan, Guangfu Ma, Chuanjiang Li*, and Boyan Jiang

Department of Control Science and Engineering, Harbin Institute of Technology, Harbin 150001, China

**Abstract:** The output feedback control for spacecraft attitude tracking system is investigated in this study. It is assumed that angular velocity measurements are not available for feedback control. A technique named adding power integrator (API) is adopted to estimate the pseudo-angular-velocity. Then we design a finite-time attitude control law, which only utilizes the relative attitude information. The stability analyses of the feedback system are proved as well, which shows the attitude tracking errors will converge into a region of zero even the external disturbances exist. The simulation results illustrate the high precision and robust attitude control performance of the proposed control strategy.

**Keywords:** output feedback, spacecraft attitude stabilization, finite-time control.

**DOI:** 10.21629/JSEE.2017.06.15

## 1. Introduction

The ability to track a desired attitude is essential for many space missions such as autonomous deployment, assembly of international space station, manipulation and repair. Take autonomous rendezvous for example, in order to successfully docking with a tumbling target or a target out of control, the docking port of the chasing spacecraft must be in alignment with that of the target as they are carrying out close-distance rendezvous and docking. Whether the space mission can succeed or not depends on the highly precise and robust relative attitude control [1]. Moreover, there are some influential factors that affect the control performance including coupling and nonlinearity of the system, uncertainties in model parameters and external disturbances and so on. Hence, the research on attitude tracking control of spacecraft is a very necessary, challenging and interesting mathematical problem of great practical importance. An amount of nonlinear control methods, such as adaptive control [2], sliding mode control [3], optimal control [4], disturbance observer-based control [5], and backstepping control [6], have been developed because the linearity control methods cannot figure out these problems.

Most of current research on spacecraft attitude tracking control is asymptotically stable, which means that the system states reach zero or desired states within infinite time. In comparison, finite-time controllers enable the system states to converge to zero in finite time, which further provides higher precision performance. Furthermore, the finite-time control method makes the system converge faster and have better robustness to disturbances because of the homogeneousness power tuning parameters in the controller. To be specific, there are two basic methods to realize finite-time control, one is the homogeneous approach [7], and the other is the Lyapunov based approach [8]. Compared with the Lyapunov based approach, the homogeneous approach cannot be applied on systems that contain uncertainties and disturbances. Also, the homogeneous approach fails to give the estimation of the settling time. For the Lyapunov based approach, it contains two branches: terminal sliding mode control (TSMC) [9] method and adding power integrator (API) [10]. One thing should be mentioned that TSMC needs to know the initial states of system and the corresponding value when the states first reach sliding mode surface to estimate the settling time. Hence API is the best finite-time methods when the settling time is required. According to current research, all the finite-time control methods have been utilized to design an attitude controller, such as the homogeneous approach in [11] and [12], API in [13] and [14], TSMC in [15] and [16] and so on.

There is some existing research on finite-time control for spacecraft attitude, and most of them have to know both the attitude and angular velocity information of spacecraft. However, it is difficult to obtain the accurate angular velocity information in the practical engineering in case of sensors fault and heavy nose. Moreover, it is valuable to do research on the angular-velocity-free controller from the perspective of cost of the whole spacecraft attitude con-

Manuscript received October 10, 2016.
*Corresponding author.
This work was supported by the National Natural Science Foundation of China (61673135; 61403103; 61603114).

trol system. For instance, the Hubble space telescope is equipped with six gyroscopes to acquire its angular velocity. In 2009, all six of the gyroscopes were replaced, among which three are used as backups, and the cost generated is hugely high. Therefore, it is conceivable to reduce the cost and ensure reliability of a spacecraft mission despite the failure of gyroscopes when output feedback attitude controllers are used without angular velocity measurements. There are three kinds of methods to realize finite-time output feedback control including homogeneous observer (HO) [17], terminal sliding mode observer (TSMO) [18] and adding power integrator filter (APIF) [19]. The first method HO is unable to estimate the upper bound of the settling time and cannot deal with disturbances as well. Moreover, both HO and TSMO have the assumption that the observation errors have constraints. In comparison with the two observer-based method, APIF can estimate the time and has no need for the boundness of observation errors. Thus, APIF may be the best choice to design an output feedback controller when the time and conservation assumption are considered. Currently, there is some research about angular-velocity-free controller based on HO and TSMO, such as HO in [20] and [21], TSMO in [22] and [23] and so on.

In this article, we investigate the problem of finite-time control for spacecraft without angular velocity information and take the external disturbances into consideration. Inspired by [19], we design an APIF to estimate the pseudo angular velocity, then a novel output feedback control method is designed. The stability of the closed-loop system is proved by strict proof, which means the system will reach a neighborhood of zero within finite time, even external disturbances exist. Compared with designing a finite-time controller for double-integrator system [19], it is more challenging to design a finite-time controller for spacecraft attitude tracking system because of the strong nonlinearity and coupling in the model.

This paper is organized as follows. The relative attitude dynamics using the unit quaternion kinematic representation and related lemmas are introduced in Section 2, which is followed by the main contribution of this paper in Section 3, then numerical simulations are given in Section 4. The final part is concluding remarks in Section 5.

**Notation:** In this paper, $\|\cdot\|$ is utilized to represent the induced norm of matrices and the Euclidean norm of vectors. For a given vector, $\boldsymbol{x} = [x_1, x_2, x_3]^{\mathrm{T}} \in \mathbf{R}^3$, define, $\mathrm{sig}(\boldsymbol{x})^{\alpha} = [|x_1|^{\alpha}\mathrm{sgn}(x_1),\ |x_2|^{\alpha}\mathrm{sgn}(x_2),\ |x_3|^{\alpha}\mathrm{sgn}(x_3)]^{\mathrm{T}}$, where $\alpha \in \mathbf{R}$.

## 2. Background and preliminaries

### 2.1 Relative attitude dynamics

In this paper, the attitude of the spacecraft is represented by the unit quaternion, which is free of singularity. $(\boldsymbol{q}, q_0) \in \mathbf{R}^3 \times \mathbf{R}$ and $(\boldsymbol{q_t}, q_{t0}) \in \mathbf{R}^3 \times \mathbf{R}$ respectively represent the body frame's orientation and the target frame relative to the inertial frame. $\boldsymbol{\omega} \in \mathbf{R}^3$ and $\boldsymbol{\omega_t} \in \mathbf{R}^3$ respectively represent the angular velocity of the chasing spacecraft and the target body frame which are expressed in their respective body frame. The relative attitude error $(\boldsymbol{q_e}, q_{e0}) \in \mathbf{R}^3 \times \mathbf{R}$ and the relative angular velocity error $\boldsymbol{\omega_e}$ are given [24] as follows:

$$\begin{cases} \boldsymbol{q_e} = q_{t0}\boldsymbol{q} - q_0\boldsymbol{q_t} + \boldsymbol{q}^{\times}\boldsymbol{q_t} \\ q_{e0} = q_{t0}q_0 + \boldsymbol{q_t}^{\mathrm{T}}\boldsymbol{q} \end{cases} \tag{1}$$

$$\boldsymbol{\omega_e} = \boldsymbol{\omega} - \tilde{\boldsymbol{R}}\boldsymbol{\omega_t} \tag{2}$$

where $\tilde{\boldsymbol{R}} \in \mathbf{R}^{3\times3}$ is the rotation matrix used to transform the target body frame to the chaser body frame and is given by

$$\tilde{\boldsymbol{R}} = (q_{e0}^2 - \boldsymbol{q_e}^{\mathrm{T}}\boldsymbol{q_e})\boldsymbol{I}_3 + 2\boldsymbol{q_e}\boldsymbol{q_e}^{\mathrm{T}} - 2q_{e0}\boldsymbol{q_e}^{\times} \tag{3}$$

where $\boldsymbol{I}_3$ is a $3\times3$ identity matrix. For any vector $\boldsymbol{c} = [c_1, c_2, c_3]^{\mathrm{T}}$, the symbol $\boldsymbol{c}^{\times}$ refers to a matrix, that is

$$\boldsymbol{c}^{\times} = [0, -c_3, c_2; c_3, 0, -c_1; -c_2, c_1, 0]. \tag{4}$$

Then the relative kinematic equation and relative dynamic equation are described [25] by

$$\begin{aligned} &\dot{\boldsymbol{q}}_e = \boldsymbol{Q}\boldsymbol{\omega}_e, \quad \dot{q}_{e0} = -0.5\boldsymbol{q_e}^{\mathrm{T}}\boldsymbol{\omega_e} \\ &\boldsymbol{J}\dot{\boldsymbol{\omega}}_e = -\boldsymbol{\omega}^{\times}\boldsymbol{J}\boldsymbol{\omega} + \boldsymbol{J}(\boldsymbol{\omega_e}^{\times}\tilde{\boldsymbol{R}}\boldsymbol{\omega_t} - \tilde{\boldsymbol{R}}\dot{\boldsymbol{\omega}}_t) + \boldsymbol{\tau} + \boldsymbol{d} \end{aligned} \tag{5}$$

where the attitude matrix $\boldsymbol{Q}$ can be written as

$$\boldsymbol{Q} = 0.5\boldsymbol{q_e}^{\times} + 0.5q_{e0}\boldsymbol{I}_3. \tag{6}$$

$\boldsymbol{J} = \boldsymbol{J}^{\mathrm{T}}$ and $\boldsymbol{d}$ are the positive definite inertia matrix and external disturbance respectively. $\boldsymbol{\tau} \in \mathbf{R}^3$ is the control torque with three axles vertical to each other.

Define $\dot{\boldsymbol{\sigma}}_e = \boldsymbol{v}$, and the relative kinematic equation and rela-
tive dynamic equation can be written as

$$\begin{cases} \dot{\boldsymbol{q}}_e = \boldsymbol{v} \\ \dot{\boldsymbol{v}} = \boldsymbol{f}(\boldsymbol{q_e}, \boldsymbol{v}) + \boldsymbol{Q}\boldsymbol{J}^{-1}\boldsymbol{\tau} \end{cases} \tag{7}$$

where $\boldsymbol{f}(\boldsymbol{q_e}, \boldsymbol{v})$ can be constructed as follows:

$$\begin{aligned} \boldsymbol{f}(\boldsymbol{q_e}, \boldsymbol{v}) = {} & \dot{\boldsymbol{Q}}\boldsymbol{Q}^{-1}\boldsymbol{v} - \boldsymbol{Q}\boldsymbol{J}^{-1}(\boldsymbol{Q}^{-1}\boldsymbol{v} + \tilde{\boldsymbol{R}}\boldsymbol{\omega_t})^{\times}\boldsymbol{J}(\boldsymbol{Q}^{-1}\boldsymbol{v} + \\ & \tilde{\boldsymbol{R}}\boldsymbol{\omega_t}) + \boldsymbol{Q}[(\boldsymbol{Q}^{-1}\boldsymbol{v})^{\times}\tilde{\boldsymbol{R}}\boldsymbol{\omega_t} - \tilde{\boldsymbol{R}}\dot{\boldsymbol{\omega}}_t] + \boldsymbol{Q}\boldsymbol{J}^{-1}\boldsymbol{d}. \end{aligned} \tag{8}$$

Note that $\|\boldsymbol{Q}\| \leqslant 1$ and $\|\tilde{\boldsymbol{R}}\| \leqslant 1$ [25], then $\boldsymbol{f}(\boldsymbol{q_e}, \boldsymbol{v})$ is constrained by

$$\begin{aligned} \|\boldsymbol{f}(\boldsymbol{q_e}, \boldsymbol{v})\| \leqslant {} & a_1(\boldsymbol{q_e})\|\boldsymbol{v}\|^2 + a_2(\boldsymbol{q_e}, \boldsymbol{\omega_t})\|\boldsymbol{v}\| + \\ & a_3(\boldsymbol{q_e}, \boldsymbol{\omega_t}, \dot{\boldsymbol{\omega}}_t, \boldsymbol{d}) \end{aligned} \tag{9}$$

where $a_1(\boldsymbol{q_e}) = 0.5\|\boldsymbol{Q}^{-1}\| + 1.25\|\boldsymbol{Q}^{-1}\|^2$, $a_2(\boldsymbol{q_e}, \boldsymbol{\omega_t}) = 3\|\boldsymbol{Q}^{-1}\|\|\boldsymbol{\omega_t}\|$, and $a_3(\boldsymbol{\omega_t}, \dot{\boldsymbol{\omega}}_t, \boldsymbol{d}) = \|\boldsymbol{J}^{-1}\|\|\boldsymbol{d}\| + \|\boldsymbol{\omega_t}\|^2 + \|\dot{\boldsymbol{\omega}}_t\|$.

**Assumption 1** The disturbance $\boldsymbol{d}$ and the target spacecraft angular velocity $\boldsymbol{\omega_t}$ as well as its first derivative $\dot{\boldsymbol{\omega}}_{\boldsymbol{t}}$ are bounded all the time. We assume that

$$\|\boldsymbol{J}^{-1}\|\|\boldsymbol{d}\| + \|\boldsymbol{\omega_t}\|^2 + \|\dot{\boldsymbol{\omega}}_{\boldsymbol{t}}\| \leqslant l$$

where $l$ is a positive constant.

**Assumption 2** Suppose that $q_{e0} \neq 0$ all the time.

Based on Assumption 2, the attitude matrix $\boldsymbol{Q}$ is invertible and $\boldsymbol{Q}^{-1}$ is nonsingular.

As in Assumption 1, the constraint of $\boldsymbol{f}(\boldsymbol{q_e}, \boldsymbol{v})$ in (9) can be transformed into

$$\|\boldsymbol{f}(\boldsymbol{q_e}, \boldsymbol{v})\| \leqslant a_4(\boldsymbol{q_e})(\|\boldsymbol{v}\|^2 + \|\boldsymbol{v}\|) + l \tag{10}$$

where $a_4(\boldsymbol{q_e}) = \max\{a_1(\boldsymbol{q_e}), a_2(\boldsymbol{q_e})\}$.

### 2.2 Lemmas

Take the following system as an example:

$$\dot{\boldsymbol{x}}(t) = \boldsymbol{f}(\boldsymbol{x}(t)), \quad \boldsymbol{x} \in \mathbf{R}^n \tag{11}$$

where $\boldsymbol{f} : U_0 \to \mathbf{R}^n$. Assume that the system in (11) satisfies the uniqueness principle of solution for all initial values forward in time.

**Lemma 1** (Bhat et al. [8]) For the system expressed as (11). Assume that there exist a candidate Lyapunov function $V$, positive constants $m \in (0, 1)$ and $h > 0$. If $\dot{V} + hV^m < 0$, the origin of (11) is finite-time stable, and the corresponding settling time can be calculated by $T \leqslant |V_0|^{1-m}/[h(1-m)]$, where $V_0$ is the initial condition of $V(\boldsymbol{x})$.

**Lemma 2** (Qian et al. [10]) Consider any $y \in \mathbf{R}, x \in \mathbf{R}$, $m \in \mathbf{R}^+$ and $n \in \mathbf{R}^+$, then the following inequality can be proved.

$$|x|^n|y|^m \leqslant (n|x|^{n+m} + m|y|^{n+m})/(n+m)$$

**Lemma 3** (Du et al. [26]) For any $x_i \in \mathbf{R}$ $(i = 1, 2, \ldots, n)$, and a real number $p \in (0, 1]$, the following inequality holds:

$$(|x_1| + \cdots + |x_n|)^p \leqslant |x_1|^p + \cdots + |x_n|^p \leqslant$$

$$n^{1-p}(|x_1| + \cdots + |x_n|)^p.$$

## 3. Finite-time output feedback attitude tracking controller design

To achieve attitude tracking control without measuring the angular velocity, (i.e., $\boldsymbol{\omega}$ and $\dot{\boldsymbol{q}}_{\boldsymbol{e}}$ are not required), we design an observer to estimate the velocity level states, then a velocity-measurement-free controller is derived by using the estimated signals, and finally a Lyapunov direct stability theorem is utilized to demonstrate the finite-time stability.

Let $\hat{\boldsymbol{v}}$ be the estimate of $\boldsymbol{v}$ (i.e. $\dot{\boldsymbol{q}}_{\boldsymbol{e}}$), then the proposed observer and output feedback controller for system (7) are given as follows, respectively:

$$\hat{\boldsymbol{v}} = \mathrm{sig}(\boldsymbol{z} + a_5\boldsymbol{q_e})^{\frac{1}{g}}, \quad \dot{\boldsymbol{z}} = -a_5\hat{\boldsymbol{v}} \tag{12}$$

$$\boldsymbol{\tau} = -a_6\boldsymbol{J}\boldsymbol{Q}^{-1}\mathrm{sig}[\mathrm{sig}(\hat{\boldsymbol{v}})^g + a_7^g\boldsymbol{q_e}]^{-1+\frac{2}{g}} \tag{13}$$

where $a_5$, $a_6$, $a_7$ and $g \in (1, 2)$ are positive constants which can be tuned to change the performance for the observer as well as the controller, and will be detailedly given in the later part of the following proof.

Then the primary contribution of this paper is presented as follows:

**Theorem 1** Consider the attitude dynamics described by (7) under observer (12) and output controller (13). Under the condition of Assumptions 1 and 2 holding, the observation errors and tracking errors can reach a neighborhood of zero within finite time. The settling time and the boundness on observer errors as well as tracking errors will be presented in the following.

**Proof** We define a candidate Lyapunov function as

$$V = V_1 + V_2 + V_3 \tag{14}$$

$$V_1 = \boldsymbol{q_e}^{\mathrm{T}}\boldsymbol{q_e}, \quad V_2 = \sum_{i=1}^{3} V_{2i}, \quad V_3 = \boldsymbol{e}^{\mathrm{T}}\boldsymbol{e} \tag{15}$$

where $V_{2i} = \displaystyle\int_{v_i^*}^{v_i} -\mathrm{sig}[\mathrm{sig}(v_i^*)^g - \mathrm{sig}(s)^g]^{\frac{2g-1}{g}}\mathrm{d}s$, auxiliary variable $\boldsymbol{v}^* = -a_7\mathrm{sig}(\boldsymbol{q_e})^{\frac{1}{g}}$ and the observer error

$$\boldsymbol{e} = \mathrm{sig}(\boldsymbol{v})^g - \mathrm{sig}(\hat{\boldsymbol{v}})^g = -\boldsymbol{z} - a_5\boldsymbol{q_e} + \mathrm{sig}(\boldsymbol{v})^g. \tag{16}$$

Then a new auxiliary variable is introduced here

$$\boldsymbol{\xi} = \mathrm{sig}(\boldsymbol{v})^g - \mathrm{sig}(\boldsymbol{v}^*)^g. \tag{17}$$

According to Lemma A.1 in [10], we have

$$|v_i - v_i^*| \leqslant 2^{1-\frac{1}{g}}|\xi_i|^{\frac{1}{g}}. \tag{18}$$

Taking the derivative of $V_1$ in (15) and applying (18), we can show that

$$\dot{V}_1 \leqslant -2a_7\sum_{i=1}^{3}|q_{ei}|^{1+\frac{1}{g}} + 2^{2-\frac{1}{g}}\sum_{i=1}^{3}q_{ei}|\xi_i|^{\frac{1}{g}}. \tag{19}$$

According to Lemma 3, (20) can be written as

$$\dot{V}_1 = -2a_7\sum_{i=1}^{3}|q_{ei}|^{1+\frac{1}{g}} + a_8\sum_{i=1}^{3}|q_{ei}|^{1+\frac{1}{g}} +$$

$$a_9\sum_{i=1}^{3}|\xi_i|^{1+\frac{1}{g}} \tag{20}$$

where $a_8 = 2^{2-\frac{1}{g}}g/(1+g)$ and $a_9 = 2^{2-\frac{1}{g}}/(1+g)$.

Calculate the derivative of $V_{2i}$ in (15) and refer to the same lines in [10], it can be shown that

$$\dot{V}_{2i} = (2-\frac{1}{g})\int_{v_i^*}^{v_i} \mathrm{sig}[\mathrm{sig}(s)^g - \mathrm{sig}(v_i^*)^g]^{\frac{g-1}{g}}\mathrm{d}s\cdot \frac{\mathrm{d}[\mathrm{sig}(v_i^*)^g]}{\mathrm{d}t} + \mathrm{sig}(\xi_i)^{\frac{2g-1}{g}}\dot{v}_i. \tag{21}$$

Making use of this result in (18) and calculating the derivative of $\mathrm{sig}(v_i^*)^g$, we obtain that

$$|v_i| \leqslant |v_i - v_i^*| + |v_i^*| \leqslant 2^{1-\frac{1}{g}}|\xi_i|^{g^{-1}} + a_7|q_{ei}|^{g^{-1}} \tag{22}$$

$$\frac{\mathrm{d}[\mathrm{sig}(v_i^*)^g]}{\mathrm{d}t} = -a_7^g v_i. \tag{23}$$

Substituting (22) and (23) into (21) yields

$$\left(2-\frac{1}{g}\right)\int_{v_i^*}^{v_i} \mathrm{sig}[\mathrm{sig}(s)^g - \mathrm{sig}(v_i^*)^g]^{\frac{g-1}{g}}\mathrm{d}s\frac{\mathrm{d}[\mathrm{sig}(v_i^*)^g]}{\mathrm{d}t} \leqslant \left(2-\frac{1}{g}\right)|\xi_i|^{\frac{g-1}{g}}\left|\frac{\mathrm{d}[\mathrm{sig}(v_i^*)^g]}{\mathrm{d}t}\right||v-v^*| \leqslant 2^{\frac{g-1}{g}}\left(2-\frac{1}{g}\right)a_7^g|\xi_i|v_i \leqslant 2^{-\frac{1}{g}+1}\left(2-\frac{1}{g}\right)a_7^g|\xi_i|\left(2^{-\frac{1}{g}+1}|\xi_i|^{\frac{1}{g}} + a_7|q_{ei}|^{\frac{1}{g}}\right) \leqslant a_{10}|q_{ei}|^{1+\frac{1}{g}} + a_{11}|\xi_i|^{1+\frac{1}{g}} \tag{24}$$

where Lemma 3 is used. $a_{10}$ and $a_{11}$ are as follows: $a_{10} = 2^{1-\frac{1}{g}}\left(2-\frac{1}{g}\right)a_7^{g+1}/(1+g)$, and $a_{11} = 2^{1-\frac{1}{g}}\left(2-\frac{1}{g}\right)a_7^g\left(a_7^g + 2^{1-\frac{1}{g}}\right)/(1+g)$.

Substituting (7) into (21) yields

$$\mathrm{sig}(\xi_i)^{\frac{2g-1}{g}}\dot{v}_i = \mathrm{sig}(\xi_i)^{-\frac{1}{g}+2}f(\boldsymbol{q}_e,\boldsymbol{v})_i + \mathrm{sig}(\xi_i)^{-\frac{1}{g}+2}(\boldsymbol{QJ}^{-1}\boldsymbol{\tau})_i. \tag{25}$$

It can be further obtained from (9) that

$$|\boldsymbol{f}(\boldsymbol{q_e},\boldsymbol{v})_i| \leqslant a_4(\boldsymbol{q_e})\left(\sum_{l=1}^3 v_l^2 + \sum_{l=1}^3 |v_l|\right) + l. \tag{26}$$

For spacecraft in realistic scenarios, the value of $\boldsymbol{v}$ will not surpass 1, then (26) can be reduced to

$$|\boldsymbol{f}(\boldsymbol{q_e},\boldsymbol{v})_i| \leqslant 2a_4\sum_{l=1}^3 |v_l|^{2-g} + l. \tag{27}$$

Inserting (27) into (25) yields

$$\mathrm{sig}(\xi_i)^{-\frac{1}{g}+2}\boldsymbol{f}(\boldsymbol{q_e},\boldsymbol{v})_i \leqslant 2a_4|\xi_i|^{-\frac{1}{g}+2}\sum_{l=1}^3 |v_l|^{-g+2} + l|\xi_i|^{-\frac{1}{g}+2}. \tag{28}$$

The term $|\xi_i|^{2-\frac{1}{g}}|v_l|^{2-g}$ in (28), in terms of (22) and Lemma 2 and Lemma 4, can be written as

$$|\xi_i|^{2-\frac{1}{g}}|v_l|^{-g+2} \leqslant |\xi_i|^{2-\frac{1}{g}}(a_7^{2-g}|q_{el}|^{\frac{2-g}{g}} + 2^{\frac{3g-g^2-2}{g}}|\xi_l|^{\frac{2-g}{g}}) \leqslant a_{12}|q_{el}|^{\frac{g+1}{g}} + a_{13}|\xi_l|^{\frac{g+1}{g}} + a_{14}|\xi_i|^{\frac{g+1}{g}} \tag{29}$$

where $a_{12} = a_7^{2-g}(2-g)(1+g)^{-1}$, $a_{13} = 2^{\frac{3g-g^2-2}{g}}(2-g)(1+g)^{-1}$, and $a_{14} = (2g-1)[a_7^{2-g}+2^{\frac{3g-g^2-2}{g}}]/(1+g)$.

Substitution of (29) into (28) leads to

$$\mathrm{sig}(\xi_i)^{-\frac{1}{g}+2}\boldsymbol{f}(\boldsymbol{q_e},\boldsymbol{v})_i \leqslant 2a_4a_{12}\sum_{l=1}^3 |q_{el}|^{1+\frac{1}{g}} + 2a_4a_{13}\sum_{l=1}^3 |\xi_l|^{1+\frac{1}{g}} + 6a_4a_{14}|\xi_i|^{\frac{1}{g}+1} + l|\xi_i|^{-\frac{1}{g}+2} \tag{30}$$

Putting together (21), (24) and (30) yields

$$\dot{V}_{2i} \leqslant a_{10}|q_{ei}|^{1+\frac{1}{g}} + 2a_4a_{12}\sum_{l=1}^3 |q_{el}|^{\frac{1}{g}+1} + a_{11}|\xi_i|^{\frac{1}{g}+1} + 2a_4a_{13}\sum_{l=1}^3 |\xi_l|^{\frac{1}{g}+1} + 6a_4a_{14}|\xi_i|^{\frac{1}{g}+1} + l|\xi_i|^{\frac{2g-1}{g}} + \mathrm{sig}(\xi_i)^{\frac{2g-1}{g}}(\boldsymbol{QJ}^{-1}\boldsymbol{\tau})_i \tag{31}$$

Now by substituting (31), $\dot{V}_2 = \sum_{i=1}^3 \dot{V}_{2i}$ can be written as

$$\dot{V}_2 \leqslant (a_{10} + 6a_7a_{12})\sum_{i=1}^3 |q_{ei}|^{1+\frac{1}{g}} + [a_{11} + 6a_4(a_{13}+a_{14})]\cdot\sum_{i=1}^3 |\xi_i|^{\frac{g+1}{g}} + l\sum_{i=1}^3 |\xi_i|^{-\frac{1}{g}+2} + \sum_{i=1}^3 \mathrm{sig}(\xi_i)^{-\frac{1}{g}+2}(\boldsymbol{QJ}^{-1}\boldsymbol{\tau})_i. \tag{32}$$

Taking the derivative of $V_3$ in (15) and applying (7), (12) and (16) yield

$$\dot{V}_3 = 2\boldsymbol{e}^{\mathrm{T}}\dot{\boldsymbol{e}} = 2g\boldsymbol{e}^{\mathrm{T}}\mathrm{diag}(|\boldsymbol{v}|^{g-1})\dot{\boldsymbol{v}} + 2a_5\boldsymbol{e}^{\mathrm{T}}\hat{\boldsymbol{v}} - 2a_5\boldsymbol{e}^{\mathrm{T}}\boldsymbol{v} = 2g\boldsymbol{e}^{\mathrm{T}}\mathrm{diag}(|\boldsymbol{v}|^{g-1})[\boldsymbol{f}(\boldsymbol{q_e},\boldsymbol{v}) + \boldsymbol{QJ}^{-1}\boldsymbol{\tau}] + 2a_5\boldsymbol{e}^{\mathrm{T}}\mathrm{sig}[\mathrm{sig}(\boldsymbol{v})^g - \boldsymbol{e}]^{\frac{1}{g}} - 2a_5\boldsymbol{e}^{\mathrm{T}}\boldsymbol{v} = 2g\sum_{i=1}^3 e_i|v_i|^{g-1}\boldsymbol{f}(\boldsymbol{q_e},\boldsymbol{v})_i + 2g\sum_{i=1}^3 e_i|v_i|^{g-1}(\boldsymbol{QJ}^{-1}\boldsymbol{\tau})_i - 2a_5\sum_{i=1}^3\{e_iv_i + e_i\mathrm{sig}[e_i - \mathrm{sig}(v_i)^g]^{\frac{1}{g}}\}. \tag{33}$$

Inserting (27) into the right side of (33) yields

$$2g\sum_{i=1}^{3} e_i|v_i|^{g-1}\boldsymbol{f}(\boldsymbol{q_e},\boldsymbol{v})_i \leqslant$$
$$4a_4g\sum_{i=1}^{3}\left[|e_i||v_i|^{g-1}\left(\sum_{l=1}^{3}|v_l|^{2-g}\right)\right]+$$
$$2gl\sum_{i=1}^{3}(|e_i||v_i|^{g-1}). \tag{34}$$

Using Lemma 2 we rewrite $|e_i||v_i|^{g-1}|v_l|^{2-g}$ in (34) as

$$|e_i||v_i|^{g-1}|v_l|^{2-g} \leqslant (g-1)|e_i||v_l|+(2-g)|e_i||v_l|. \tag{35}$$

By imposing (22), according to Lemma 2, the above inequation has the following new form:

$$|e_i||v_i|^{g-1}|v_l|^{-g+2} \leqslant$$
$$2^{\frac{g-1}{g}}(g-1)|e_i||\xi_i|^{g^{-1}} + a_7(g-1)|e_i||q_{ei}|^{g^{-1}}+$$
$$2^{\frac{g-1}{g}}(2-g)|e_i||\xi_l|^{g^{-1}} + a_7(2-g)|e_i||q_{el}|^{g^{-1}} \leqslant$$
$$a_{15}|q_{ei}|^{1+\frac{1}{g}} + a_{16}|q_{el}|^{1+\frac{1}{g}} + a_{17}|\xi_i|^{1+\frac{1}{g}}+$$
$$a_{18}|\xi_l|^{1+\frac{1}{g}} + a_{19}|e_i|^{1+\frac{1}{g}} \tag{36}$$

where $a_{15} = a_7(g-1)(1+g)^{-1}$, $a_{16} = a_7(2-g)(1+g)^{-1}$, $a_{17} = 2^{1-\frac{1}{g}}(g-1)(1+g)^{-1}$, $a_{18} = 2^{1-\frac{1}{g}}(2-g)(1+g)^{-1}$, and $a_{19} = (2^{1-\frac{1}{g}} + a_7)g(1+g)^{-1}$.

Substitution of (36) into (34) yields

$$4a_4g\sum_{i=1}^{3}[|e_i||v_i|^{g-1}(\sum_{l=1}^{3}|v_l|^{2-g})] \leqslant$$
$$12a_4g(a_{15}+a_{16})\sum_{i=1}^{3}|q_{ei}|^{1+\frac{1}{g}} + 12a_4g(a_{17}+a_{18})\cdot$$
$$\sum_{i=1}^{3}|\xi_i|^{\frac{1}{g}+1} + 12a_4a_{19}g\sum_{i=1}^{3}|e_i|^{\frac{1}{g}+1}. \tag{37}$$

According to (22) and Lemma 3, we obtain

$$|v_i|^{g-1} \leqslant 2^{g^{-1}-2+g}|\xi_i|^{\frac{g-1}{g}} + a_7^{g-1}|q_{ei}|^{\frac{g-1}{g}}. \tag{38}$$

Using (38) and Lemma 2, (34) becomes

$$2g\bar{d}\sum_{i=1}^{3}|e_i||v_i|^{g-1} \leqslant 2^{g-1+\frac{1}{g}}g\bar{d}\sum_{i=1}^{3}|e_i||\xi_i|^{-\frac{1}{g}+1}+$$
$$2a_7^{g-1}g\bar{d}\sum_{i=1}^{3}e_i|q_{ei}|^{\frac{g-1}{g}} \leqslant a_{20}\sum_{i=1}^{3}|q_{ei}|^{\frac{g-1}{g}}+$$
$$a_{21}\sum_{i=1}^{3}|\xi_i|^{\frac{g-1}{g}} + a_{22}\sum_{i=1}^{3}|e_i|^{\frac{2g-1}{g}} \tag{39}$$

where $a_{20} = 2a_7^{g-1}g(g-1)l(2g-1)^{-1}$, $a_{21} = 2^{g-1+\frac{1}{g}}g(g-1)l(2g-1)^{-1}$, and $a_{22} = (2^{g-1+\frac{1}{g}}+2)g^2l(2g-1)^{-1}$.

Now by substituting (37) and (39), (34) can be written as

$$2g\sum_{i=1}^{3}e_i|v_i|^{g-1}\boldsymbol{f}(\boldsymbol{q_e},\boldsymbol{v})_i \leqslant 12a_4g(a_{15}+a_{16})\sum_{i=1}^{3}|q_{ei}|^{\frac{1}{g}+1}+$$
$$12a_4g(a_{17}+a_{18})\sum_{i=1}^{3}|\xi_i|^{\frac{g+1}{g}} + 12a_4a_{19}g\sum_{i=1}^{3}|e_i|^{\frac{g+1}{g}}+$$
$$a_{20}\sum_{i=1}^{3}|q_{ei}|^{\frac{2g-1}{g}} + a_{21}\sum_{i=1}^{3}|\xi_i|^{\frac{2g-1}{g}} + a_{22}\sum_{i=1}^{3}|e_i|^{\frac{2g-1}{g}}. \tag{40}$$

According to Lemma 2, (33) can be written into

$$2g\sum_{i=1}^{3}e_i|v_i|^{g-1}(\boldsymbol{QJ}^{-1}\boldsymbol{\tau})_i =$$
$$2g\sum_{i=1}^{3}e_i(|v_i|^{2-g})^{\frac{g-1}{2-g}}(\boldsymbol{QJ}^{-1}\boldsymbol{\tau})_i \leqslant$$
$$2g(g-1)\sum_{i=1}^{3}|e_i||v_i| + 2g(2-g)\sum_{i=1}^{3}|e_i||(\boldsymbol{QJ}^{-1}\boldsymbol{\tau})_i|^{\frac{1}{2-g}}. \tag{41}$$

Using (22), Lemma 2 is applied again, then the term in (41) has the following form:

$$2g(g-1)\sum_{i=1}^{3}|e_i||v_i| \leqslant 2^{2-\frac{1}{g}}g(g-1)\sum_{i=1}^{3}|e_i||\xi_i|^{\frac{1}{g}}+$$
$$2a_7g(g-1)\sum_{i=1}^{3}|e_i||q_{ei}|^{\frac{1}{g}} \leqslant a_{23}\sum_{i=1}^{3}|q_{ei}|^{\frac{g+1}{g}}+$$
$$a_{24}\sum_{i=1}^{3}|\xi_i|^{\frac{g+1}{g}} + a_{25}\sum_{i=1}^{3}|e_i|^{\frac{g+1}{g}} \tag{42}$$

where $a_{23} = 2a_7g(g-1)(1+g)^{-1}$, $a_{24} = 2^{2-\frac{1}{g}}g(g-1)(1+g)^{-1}$, and $a_{25} = (2^{2-\frac{1}{g}}+2a_7)g^2(g-1)(1+g)^{-1}$.

By defining the estimation of $\boldsymbol{\xi}$ as

$$\hat{\boldsymbol{\xi}} = \mathrm{sig}(\hat{\boldsymbol{v}})^g - \mathrm{sig}(\boldsymbol{v}^*)^g, \tag{43}$$

the observer error in (16) can be rewritten as $\boldsymbol{e} = \boldsymbol{\xi} - \hat{\boldsymbol{\xi}}$.

Then, the proposed control law in (13) has the form

$$\boldsymbol{\tau} = -a_6\boldsymbol{JQ}^{-1}\mathrm{sig}(\hat{\boldsymbol{\xi}})^{\frac{2}{g}-1} =$$
$$-a_6\boldsymbol{JQ}^{-1}\mathrm{sig}(\boldsymbol{\xi}-\boldsymbol{e})^{-1+\frac{2}{g}}. \tag{44}$$

Substituting the controller in (44), Lemma 2 and Lemma 3, we obtain the following inequality:

$$\sum_{i=1}^{3}|e_i||(\boldsymbol{QJ}^{-1}\boldsymbol{\tau})_i|^{\frac{1}{2-g}}=\sum_{i=1}^{3}|e_i||a_6\hat{\xi}_i^{\frac{2-g}{g}}|^{\frac{1}{2-g}}\leqslant$$
$$a_6\sum_{i=1}^{3}|e_i||\xi_i-e_i|^{\frac{1}{g}}\leqslant$$
$$a_6\sum_{i=1}^{3}|e_i||\xi_i|^{\frac{1}{g}}+a_6\sum_{i=1}^{3}|e_i|^{1+\frac{1}{g}}\leqslant$$
$$\frac{a_6(2g+1)}{1+g}\sum_{i=1}^{3}|e_i|^{1+\frac{1}{g}}+\frac{a_6}{1+g}\sum_{i=1}^{3}|\xi_i|^{1+\frac{1}{g}}. \tag{45}$$

Moreover, we can transform the term in (41) into the form

$$2g(2-g)\sum_{i=1}^{3}|e_i||(\boldsymbol{QJ}^{-1}\boldsymbol{\tau})_i|^{\frac{1}{2-g}}\leqslant$$
$$a_{26}\sum_{i=1}^{3}|\xi_i|^{\frac{g+1}{g}}+a_{27}\sum_{i=1}^{3}|e_i|^{\frac{g+1}{g}} \tag{46}$$

where $a_{26}=\dfrac{2a_6g(2-g)}{1+g}$ and $a_{27}=\dfrac{2a_6g(2g+1)(g-2)}{-1-g}$.

Making using of both (42) and (46), (41) is rewritten as

$$2g\sum_{i=1}^{3}e_i|v_i|^{g-1}(\boldsymbol{QJ}^{-1}\boldsymbol{\tau})_i\leqslant a_{23}\sum_{i=1}^{3}|q_{ei}|^{\frac{g+1}{g}}+$$
$$(a_{24}+a_{26})\sum_{i=1}^{3}|\xi_i|^{1+\frac{1}{g}}+(a_{25}+a_{27})\sum_{i=1}^{3}|e_i|^{1+\frac{1}{g}}. \tag{47}$$

According to Lemma 2.7 in [19], there is a positive constant $a_{28}$, then we can simplify (33) such that

$$-2a_5\sum_{i=1}^{3}\{e_iv_i+e_i\mathrm{sig}[e_i-\mathrm{sig}(v_i)^g]^{\frac{1}{g}}\}\leqslant$$
$$2a_5\sum_{i=1}^{3}|e_i|^{1+\frac{1}{g}}[-(2^{\frac{1}{g}}-1)a_{28}^{1-\frac{1}{g}}+$$
$$a_{28}^2|\mathrm{sig}(v_i)^g/e_i|^{1+\frac{1}{g}}]\leqslant$$
$$-(2^{1+\frac{1}{g}}-2)a_5a_{28}^{1-\frac{1}{g}}\sum_{i=1}^{3}|e_i|^{1+\frac{1}{g}}+2a_5a_{28}^2\sum_{i=1}^{3}|v_i|^{1+g}. \tag{48}$$

It can be further obtained from (22) and Lemma 3 that

$$|v_i|^{1+g}\leqslant 2^g(2^{g-\frac{1}{g}}|\xi_i|^{1+\frac{1}{g}}+a_7^{1+g}|q_{ei}|^{1+\frac{1}{g}}). \tag{49}$$

According to (49), (48) can be further reduced to

$$-2a_5\sum_{i=1}^{3}\{e_iv_i+e_i\mathrm{sig}[e_i-\mathrm{sig}(v_i)^g]^{\frac{1}{g}}\}\leqslant$$
$$-a_{29}\sum_{i=1}^{3}|e_i|^{1+\frac{1}{g}}+a_{30}\sum_{i=1}^{3}|q_{ei}|^{1+\frac{1}{g}}+a_{31}\sum_{i=1}^{3}|\xi_i|^{1+\frac{1}{g}} \tag{50}$$

where $a_{29}=(2^{1+\frac{1}{g}}-2)a_5a_{28}^{1-\frac{1}{g}}$, $a_{30}=2^{1+g}a_5a_7^{1+g}a_{28}^2$, and $a_{31}=2^{1+2g-\frac{1}{g}}a_5a_{28}^2$.

Now by substituting (40), (47) and (50), (33) can be rewritten as

$$\dot{V}_3\leqslant -a_{29}\sum_{i=1}^{3}|e_i|^{1+\frac{1}{g}}+$$
$$[12a_4g(a_{15}+a_{16})+a_{23}+a_{30}]\sum_{i=1}^{3}|q_{ei}|^{1+\frac{1}{g}}+$$
$$[12a_4g(a_{17}+a_{18})+a_{24}+a_{26}+a_{31}]\sum_{i=1}^{3}|\xi_i|^{1+\frac{1}{g}}+$$
$$(12a_4a_{19}g+a_{25}+a_{27})\sum_{i=1}^{3}|e_i|^{1+\frac{1}{g}}+$$
$$a_{20}\sum_{i=1}^{3}|q_{ei}|^{\frac{2g-1}{g}}+a_{21}\sum_{i=1}^{3}|\xi_i|^{\frac{2g-1}{g}}+a_{22}\sum_{i=1}^{3}|e_i|^{\frac{2g-1}{g}}. \tag{51}$$

Then the last term on the right side of (32) can be simplified further, which follows from (44) that

$$\sum_{i=1}^{3}\mathrm{sig}(\xi_i)^{\frac{2g-1}{g}}(\boldsymbol{QJ}^{-1}\boldsymbol{\tau})_i\leqslant -a_6\sum_{i=1}^{3}|\xi_i|^{\frac{g+1}{g}}+$$
$$a_6\sum_{i=1}^{3}\{\mathrm{sig}(\xi_i)^{(2g-1)g^{-1}}[\mathrm{sig}(\xi_i)^{(2-g)g^{-1}}-$$
$$\mathrm{sig}(\xi_i-e_i)^{(2-g)g^{-1}}]\}. \tag{52}$$

According to Lemma A.1 in [10], we obtain

$$\mathrm{sig}(\xi_i)^{\frac{2-g}{g}}-\mathrm{sig}(\xi_i-e_i)^{\frac{2-g}{g}}\leqslant 2^{\frac{2g-2}{g}}|e_i|^{\frac{2-g}{g}}. \tag{53}$$

Inserting (53) into (52) yields

$$\sum_{i=1}^{3}\mathrm{sig}(\xi_i)^{(2g-1)g^{-1}}(\boldsymbol{QJ}^{-1}\boldsymbol{\tau})_i\leqslant -a_6\sum_{i=1}^{3}|\xi_i|^{\frac{g+1}{g}}+$$
$$2^{(2g-1)g^{-1}}a_6\sum_{i=1}^{3}|\xi_i|^{2-\frac{1}{g}}|e_i|^{(2-g)g^{-1}}\leqslant$$
$$-a_6\sum_{i=1}^{3}|\xi_i|^{\frac{g+1}{g}}+a_{32}\sum_{i=1}^{3}|\xi_i|^{\frac{g+1}{g}}+a_{33}\sum_{i=1}^{3}|e_i|^{\frac{g+1}{g}} \tag{54}$$

where $a_{32} = 2^{2-\frac{2}{g}} a_6(2g-1)/(1+g)$ and $a_{33} = 2^{2-\frac{2}{g}} a_6(2-g)/(1+g)$.

From (54) we can rewrite $\dot{V}_2$ in (32) as

$$\dot{V}_2 \leqslant -a_6 \sum_{i=1}^{3} |\xi_i|^{1+\frac{1}{g}} + (a_{10}+6a_4a_{12}) \sum_{i=1}^{3} |q_{ei}|^{1+\frac{1}{g}} + [a_{11}+6a_4(a_{13}+a_{14})+a_{32}] \sum_{i=1}^{3} |\xi_i|^{1+\frac{1}{g}} + a_{33} \sum_{i=1}^{3} |e_i|^{\frac{g+1}{g}} + l \sum_{i=1}^{3} |\xi_i|^{\frac{2g-1}{g}}. \tag{55}$$

Take the the derivative of the candidate Lyapunov function $V = V_1 + V_2 + V_3$ for the whole system defined in (14), and substitute $\dot{V}_1$ in (20), $\dot{V}_2$ in (55) and $\dot{V}_3$ in (51). Then we can obtain

$$\dot{V} \leqslant -a_{34} \sum_{i=1}^{3} |q_{ei}|^{\frac{g+1}{g}} - a_{35} \sum_{i=1}^{3} |\xi_i|^{\frac{g+1}{g}} - a_{36} \sum_{i=1}^{3} |e_i|^{\frac{g+1}{g}} + a_{20} \sum_{i=1}^{3} |q_{ei}|^{\frac{2g-1}{g}} + (a_{21}+l) \sum_{i=1}^{3} |\xi_i|^{\frac{2g-1}{g}} + a_{22} \sum_{i=1}^{3} |e_i|^{\frac{2g-1}{g}} \tag{56}$$

where $a_{34}$, $a_{35}$ and $a_{36}$ are the positive constants satisfying the constrains as follows:

$$a_{34}=2a_7-[a_8+a_{10}+6a_4a_{12}+12a_4g(a_{15}+a_{16})+a_{23}+a_{30}$$

$$a_{35} = a_6 - [a_9 + a_{11} + 6a_4(a_{13}+a_{14}) + a_{32} + 12a_4g(a_{17}+a_{18}) + a_{24} + a_{26} + a_{31}],$$

and $a_{36} = a_{29} - [a_{33} + 12a_4a_{19}g + a_{25} + a_{27}]$.

Note that, using Lemma 3, we can transform the terms of (56) into the following forms:

$$-a_{34} \sum_{i=1}^{3} |q_{ei}|^{1+\frac{1}{g}} \leqslant -a_{34}(\boldsymbol{q_e}^{\mathrm{T}}\boldsymbol{q_e})^{\frac{1+g}{2g}} \tag{57}$$

$$-a_{35} \sum_{i=1}^{3} |\xi_i|^{1+\frac{1}{g}} \leqslant -a_{35}(\boldsymbol{\xi}^{\mathrm{T}}\boldsymbol{\xi})^{\frac{1+g}{2g}} \tag{58}$$

$$-a_{36} \sum_{i=1}^{3} |e_i|^{1+\frac{1}{g}} \leqslant -a_{36}(\boldsymbol{e}^{\mathrm{T}}\boldsymbol{e})^{\frac{1+g}{2g}} \tag{59}$$

$$a_{20} \sum_{i=1}^{3} |q_{ei}|^{2-\frac{1}{g}} \leqslant 3^{\frac{1}{2g}} a_{20}(\boldsymbol{q_e}^{\mathrm{T}}\boldsymbol{q_e})^{1-\frac{1}{2g}} \tag{60}$$

$$(a_{21}+l) \sum_{i=1}^{3} |\xi_i|^{2-\frac{1}{g}} \leqslant 3^{\frac{1}{2g}} (a_{21}+l)(\boldsymbol{\xi}^{\mathrm{T}}\boldsymbol{\xi})^{1-\frac{1}{2g}} \tag{61}$$

$$a_{22} \sum_{i=1}^{3} |e_i|^{2-\frac{1}{g}} \leqslant 3^{\frac{1}{2g}} a_{22}(\boldsymbol{e}^{\mathrm{T}}\boldsymbol{e})^{1-\frac{1}{2g}}. \tag{62}$$

Defining three positive constants $\theta_{qe} \in (0,1)$, $\theta_\xi \in (0,1)$ and $\theta_e \in (0,1)$, substituting (57)–(62) into (56) and rearranging the new inequality, we have

$$\dot{V} \leqslant -a_{34}\theta_{qe}(\boldsymbol{q_e}^{\mathrm{T}}\boldsymbol{q_e})^{\frac{1+g}{2g}} - a_{35}\theta_\xi(\boldsymbol{\xi}^{\mathrm{T}}\boldsymbol{\xi})^{\frac{1+g}{2g}} - a_{36}\theta_e(\boldsymbol{e}^{\mathrm{T}}\boldsymbol{e})^{\frac{1+g}{2g}} - 3^{\frac{1}{2g}} a_{20}(\boldsymbol{q_e}^{\mathrm{T}}\boldsymbol{q_e})^{1-\frac{1}{2g}} \cdot [\frac{(1-\theta_{qe})a_{34}}{3^{\frac{1}{2g}} a_{20}}(\boldsymbol{q_e}^{\mathrm{T}}\boldsymbol{q_e})^{\frac{2-g}{2g}} - 1] - 3^{\frac{1}{2g}}(a_{21}+l)(\boldsymbol{\xi}^{\mathrm{T}}\boldsymbol{\xi})^{1-\frac{1}{2g}}[\frac{(1-\theta_\xi)a_{35}}{3^{\frac{1}{2g}}(a_{21}+l)}(\boldsymbol{\xi}^{\mathrm{T}}\boldsymbol{\xi})^{\frac{2-g}{2g}} - 1] - 3^{\frac{1}{2g}} a_{22}(\boldsymbol{\xi}^{\mathrm{T}}\boldsymbol{\xi})^{1-\frac{1}{2g}} \cdot [\frac{(1-\theta_e)a_{36}}{3^{\frac{1}{2g}} a_{22}}(\boldsymbol{e}^{\mathrm{T}}\boldsymbol{e})^{\frac{2-g}{2g}} - 1]. \tag{63}$$

If $\boldsymbol{q_e}$, $\boldsymbol{\xi}$ and $\boldsymbol{e}$ are not in the set

$$\varOmega = \{\varOmega_{qe} \cup \varOmega_\xi \cup \varOmega_e\} \tag{64}$$

where $\varOmega_{\sigma e} = \left\{ \|\boldsymbol{q_e}\| \leqslant [\frac{3^{\frac{1}{2g}} a_{20}}{(1-\theta_{\sigma e})a_{34}}]^{\frac{g}{2-g}} \right\}$,

$$\varOmega_\xi = \left\{ \|\boldsymbol{\xi}\| \leqslant [\frac{3^{\frac{1}{2g}}(a_{21}+l)}{(1-\theta_\xi)a_{35}}]^{\frac{g}{2-g}} \right\},$$

and $\varOmega_e = \left\{ \|\boldsymbol{e}\| \leqslant [\frac{3^{\frac{1}{2g}} a_{22}}{(1-\theta_e)a_{36}}]^{\frac{g}{2-g}} \right\}$, which means $\boldsymbol{q_e}$, $\boldsymbol{\xi}$ and $\boldsymbol{e}$ satisfying

$$\boldsymbol{q_e}^{\mathrm{T}}\boldsymbol{q_e} \geqslant \{3^{\frac{1}{2g}} a_{20}/[(1-\theta_{qe})a_{34}]\}^{\frac{2g}{2-g}} \tag{65}$$

$$\boldsymbol{\xi}^{\mathrm{T}}\boldsymbol{\xi} \geqslant \{3^{\frac{1}{2g}}(a_{21}+l)/[(1-\theta_\xi)a_{35}]\}^{\frac{2g}{2-g}} \tag{66}$$

$$\boldsymbol{e}^{\mathrm{T}}\boldsymbol{e} \geqslant \{3^{\frac{1}{2g}} a_{22}/[(1-\theta_e)a_{36}]\}^{\frac{2g}{2-g}} \tag{67}$$

then (63) can be written into

$$\dot{V} \leqslant -a_{34}\theta_{qe}(\boldsymbol{q_e}^{\mathrm{T}}\boldsymbol{q_e})^{\frac{1+g}{2g}} - a_{35}\theta_\xi(\boldsymbol{\xi}^{\mathrm{T}}\boldsymbol{\xi})^{\frac{1+g}{2g}} - a_{36}\theta_e(\boldsymbol{e}^{\mathrm{T}}\boldsymbol{e})^{\frac{1+g}{2g}}. \tag{68}$$

By Lemma A.1 in [10], $V_{2i}$ in (15) can be written as

$$V_{2i} \leqslant |v_i - v_i^*||\xi_i|^{\frac{2g-1}{g}} \leqslant 2^{\frac{g-1}{g}}|\mathrm{sig}(v_i)^g - \mathrm{sig}(v_i^*)^g|^{\frac{1}{g}}|\xi_i|^{\frac{2g-1}{g}} = 2^{\frac{g-1}{g}}|\xi_i|^2. \tag{69}$$

Eventually, we can get the expression of $\dot{V}$ by substituting $V_1$, $V_3$ in (15) and $V_{2i}$ in (69) into (68)

$$\dot{V} \leqslant -a_{34}\theta_{qe}V_1^{\frac{1+g}{2g}} - 2^{\frac{1-g^2}{2g^2}} a_{35}\theta_\xi V_2^{\frac{1+g}{2g}} -$$

$$a_{36}\theta_e V_3^{\frac{1+g}{2g}} \leqslant -a_{37}V^{\frac{1+g}{2g}}. \tag{70}$$

Note constant $a_{37} = \min\{a_{34}\theta_{qe}, 2^{\frac{1-g^2}{2g^2}}a_{35}\theta_\xi, a_{36}\theta_e\}$ and Lemma 3, where $g \in (1,2)$. Then (70) is the same as Lemma 1, so we can calculate $T$ by the following equation:

$$T \leqslant \frac{2g}{a_{37}(g-1)}V_{t=0}^{\frac{g-1}{2g}}. \tag{71}$$

Furthermore, the inequalities (65)−(67) imply that $\boldsymbol{q_e}$, $\boldsymbol{\xi}$ and $\boldsymbol{e}$ will converge to the ball $\Omega$ defined in (64). Consequently, Theorem 1 holds on the basis of the analyses above and the proof is completed. □

**Remark 1** It is worth mentioning that we only prove $\boldsymbol{q_e}$ can converge to $[000]^{\mathrm{T}}$ within finite time, but ignore the state $q_{e0}$, which attributes to the fact that $q_{e0} = \pm 1$ when $\boldsymbol{q_e} = [000]^{\mathrm{T}}$. Furthermore, the two equilibriums $[\boldsymbol{q_e}^{\mathrm{T}}, q_{e0}]^{\mathrm{T}} = [0001]^{\mathrm{T}}$ and $[\boldsymbol{q_e}^{\mathrm{T}}, q_{e0}]^{\mathrm{T}} = [000-1]^{\mathrm{T}}$ in the physical space correspond to the same rotation, so we only need to guarantee that $\boldsymbol{q_e} \to [000]^{\mathrm{T}}$ in finite time [11].

**Remark 2** If the fractional power $g = 1$ in (12) and (13), the controller (13) has the form

$$\boldsymbol{\tau} = -a_6\boldsymbol{J}\boldsymbol{Q}^{-1}[\hat{\boldsymbol{v}} + a_7\boldsymbol{q_e}] \tag{72}$$

where estimation of pseudo velocity $\hat{\boldsymbol{v}}$ can be calculated by the low-pass filter: $\hat{\boldsymbol{v}} = -a_5\int\hat{\boldsymbol{v}}\mathrm{d}t + a_5\boldsymbol{q_e}$. The controller (72) is seemed as a type of asymptotically filter-based output feedback controller in [27] or [28]. However, compared with the asymptotical controller in [27] or [28], the proposed finite-time controller (13) can improve the performance owning to the fractional power $g > 1$ in (12) and (13). When $\boldsymbol{q_e}$ and $\hat{\boldsymbol{v}}$ are near zero vectors, the controller (13) is able to to provide higher accuracy and faster convergence than the asymptotical controllers, since the fractional power $g$ can increase the control torque.

## 4. Simulation results

In this section, numerical examples are presented to prove the performance of the designed controller (13). The chasing spacecraft's inertia matrix is assumed [25] to be

$$\boldsymbol{J} = \begin{bmatrix} 20 & 1.2 & 0.9 \\ 1.2 & 17 & 1.4 \\ 0.9 & 1.4 & 15 \end{bmatrix}. \tag{73}$$

The chasing spacecraft's initial conditions are selected as [29] $\boldsymbol{\omega}(0) = [0,0,0]^{\mathrm{T}}$, $\boldsymbol{q}(0) = [0.182\ 6, 0.182\ 6, 0.182\ 6]^{\mathrm{T}}$ with $q_0 = \sqrt{1-3\times(0.182\ 6)^2}$. The tumbling target spacecraft is out of control and its angular velocity is unknown by the chaser spacecraft. In the following numerical simulation, we assume that the target spacecraft is static initially and its angular velocity is $\boldsymbol{\omega_t}(t) = p(t)[1,1,1]^{\mathrm{T}}\mathrm{rad/s}$ with $p(t)$ [29] given by

$$p(t) = 0.15\cos(0.3t)(1-\mathrm{e}^{0.01t^2}) + [0.04\pi + 0.03\sin(0.3t)]t\mathrm{e}^{-0.01t^2}. \tag{74}$$

In order to highlight the performance of the developed finite-time output feedback filter-based controller, we compare it with the asymptotically output feedback filter-based controller in [28], which is designed as follows:

$$\boldsymbol{\tau} = -k_1\boldsymbol{q_e} - k_2\boldsymbol{Q}^{\mathrm{T}}\dot{\boldsymbol{z}} + (\tilde{\boldsymbol{R}}\boldsymbol{\omega})^{\times}\boldsymbol{J}\tilde{\boldsymbol{R}}\boldsymbol{\omega} + \boldsymbol{J}\tilde{\boldsymbol{R}}\dot{\boldsymbol{\omega}}_{\boldsymbol{t}} \tag{75}$$

where the estimation of pseudo velocity $\dot{\boldsymbol{z}}$ is calculated by the low-pass filter: $\dot{\boldsymbol{z}} = -k_3\boldsymbol{z} + \boldsymbol{q_e}$ and $k_i > 0$ $(i = 1,2,3)$. Then the two cases (with and without disturbances) are investigated respectively.

### 4.1 Comparison without external disturbances

In this subsection, we compare the designed controller (13) with the controller (75) in [28]. The tuning parameters of the designed controller (13) are set as $a_5 = 3$, $g = 1.2$, $a_6 = 15$ and $a_7 = 1$. The control gains of the asymptotical controller (75) are selected to be $k_1 = 50$, $k_2 = 60$ and $k_3 = 15$. Fig. 1 and Fig. 2 respectively illustrate the time response of attitude tracking errors and angular velocity tracking errors. At the steady state, the bounds on $|q_{ei}|$ and $|\omega_{ei}|$ under the proposed controller (13) are $|q_{ei}| \leqslant 1\times10^{-3}$ and $|\omega_{ei}| \leqslant 5\times10^{-4}$. The bounds on $|q_{ei}|$ and $|\omega_{ei}|$ under the controller in [28] are $|q_{ei}| \leqslant 6\times10^{-3}$ and $|\omega_{ei}| \leqslant 1\times10^{-2}$ at the steady state. In addition, it takes 12 s for the controller (13) to drive the attitude tracking errors into the steady-state regions $|q_{ei}| \leqslant 5\times10^{-4}$, while the corresponding time for the controller in [28] is 16 s. Thus, we can see that the designed finite-time controller (13) is able to to provide higher accuracy and faster convergence speed than the asymptotic controller in [28], due to an additional power $g = 1.2$ contained in (13). To compare instructively, Fig. 3 shows the change of attitude tracking errors against time, and the function is described as $\phi(t) = \|\boldsymbol{q_e}\| + k_0\|\boldsymbol{\omega_e}\|$ with $k_0 = 1$ s/rad [30]. From Fig. 3, under the designed controller (13), the bound $\phi(t) \leqslant 2\times10^{-3}$ is reached at the steady state, and the settling time is 12 s. In contrast, the ultimate bound becomes $\phi(t) < 1\times10^{-2}$ under the controller in [28], and the time for $\phi(t)$ to reach steady-state regions is 16 s. Fig. 4 illustrates the control torques of the two controllers. As is shown in the figure, the controller (13) outputs smaller control torques than that of the controller in [28]. Then we present the energy consumption of the designed controllers in Fig. 5. The energy index is defined as followed, which is decided by the energy that the actuators consume when the chasing spacecraft conduct attitude stabilization.

$$E_{\text{energy}} = \sum_{i=1}^{3} \int_0^t |\tau_i(t)|^2 \mathrm{d}t \tag{76}$$

We can see that the amount of energy consumed by the controller (13) is about two-thirds of that consumed by the controller in [28]. Consequently, the proposed controller (13) achieves faster convergence with higher accuracy, and consumes less energy than the controller in [28], due to the adjustable power gain $g$.

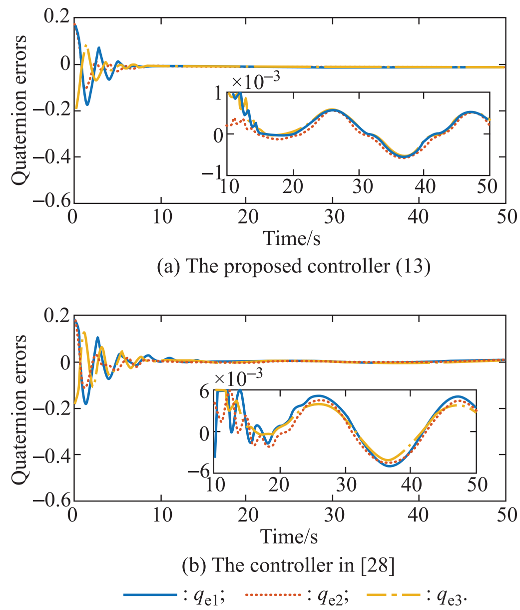

(a) The proposed controller (13)
(b) The controller in [28]

**Fig. 1 Time response of attitude tracking errors without disturbance**

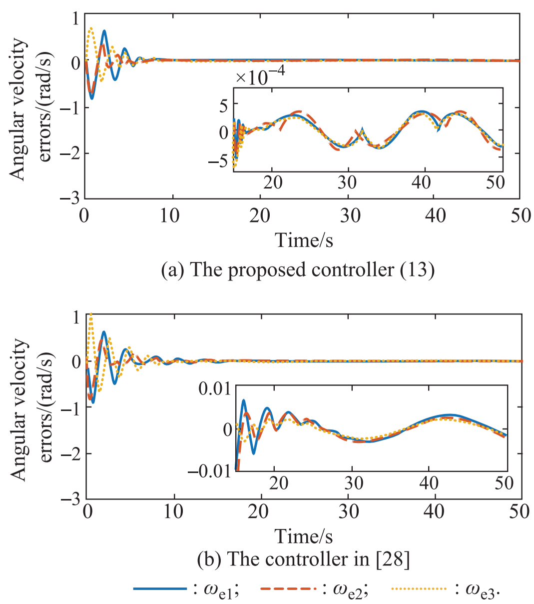

(a) The proposed controller (13)
(b) The controller in [28]

**Fig. 2 Time response of angular velocity tracking errors without disturbance**

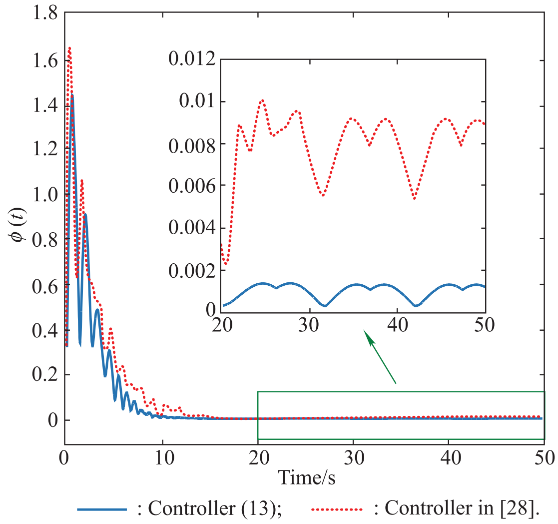


**Fig. 3 Attitude tracking errors function $\phi(t)$ without disturbance under controller (13) and controller in [28]**

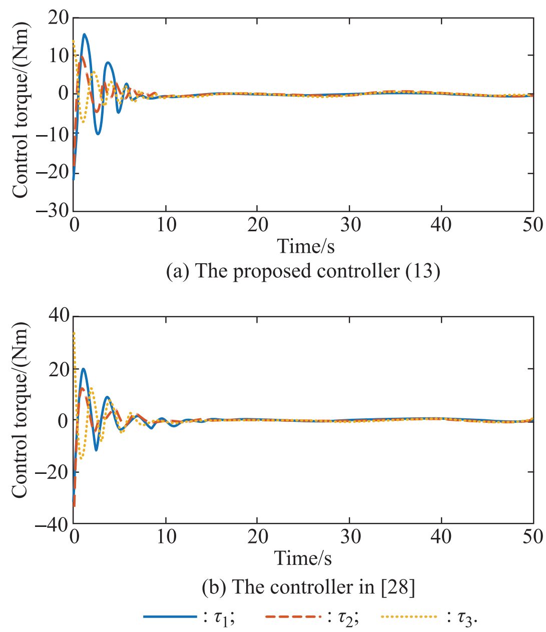

(a) The proposed controller (13)
(b) The controller in [28]

**Fig. 4 Time response of control input without disturbance**

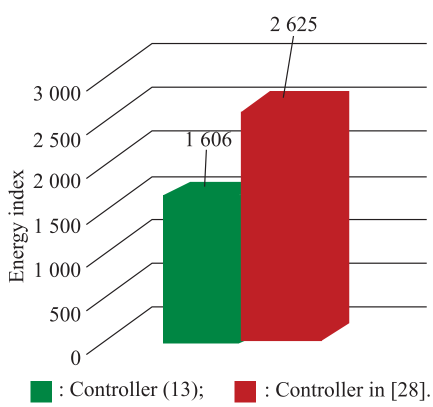


**Fig. 5 Energy index under controller (13) and controller in [28] without disturbance**

### 4.2 Comparison with disturbances

The control properties of the proposed controller (13), compared with the controller in [28] are illustrated here in the presence of external disturbance. The control gains are the same as the above subsection. Disturbances $\boldsymbol{d}(t)$ [25] is chosen as

$$\boldsymbol{d}(t) = (\|\boldsymbol{\omega}\|^2 + 0.5)[\cos(0.7t)\sin(0.4t)\sin(0.2t)]^{\mathrm{T}} + 0.01\mathrm{rand}(t) \tag{77}$$

where $\mathrm{rand}(t) \in [-1, 1]$ are zero-mean random numbers with simple time being 0.01 s. Moreover, an input delay 10 ms is also considered. The analysis procedure is similar to that in the above case. Fig. 6 and Fig. 7 show the angular velocity tracking errors and attitude tracking errors respectively. At the steady state, the bounds on $|q_{ei}|$ and $|\omega_{ei}|$ under the proposed controller (13) are $|q_{ei}| \leqslant 2 \times 10^{-3}$ and $|\omega_{ei}| \leqslant 2 \times 10^{-3}$. The bounds on $|q_{ei}|$ and $|\omega_{ei}|$ under the controller in [28] are $|q_{ei}| \leqslant 1 \times 10^{-2}$ and $|\omega_{ei}| \leqslant 2 \times 10^{-2}$ at steady state. In addition, it takes 12 s for the controller (13) to drive the attitude tracking errors into the regions $|q_{ei}| \leqslant 2 \times 10^{-3}$, while the corresponding time for controller in [28] is 13 s. From Fig. 8, under the proposed controller (13) and controller in [28], the bounds $\phi(t) \leqslant 3 \times 10^{-3}$ and $\phi(t) \leqslant 2 \times 10^{-2}$ are reached at steady state, respectively, moreover, the former one takes less time than the latter one obviously.

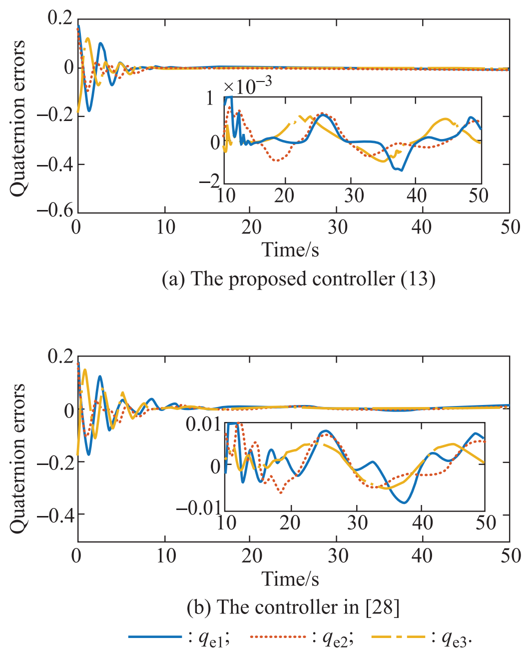

(a) The proposed controller (13)

(b) The controller in [28]

**Fig. 6 Time response of attitude tracking errors with disturbance**

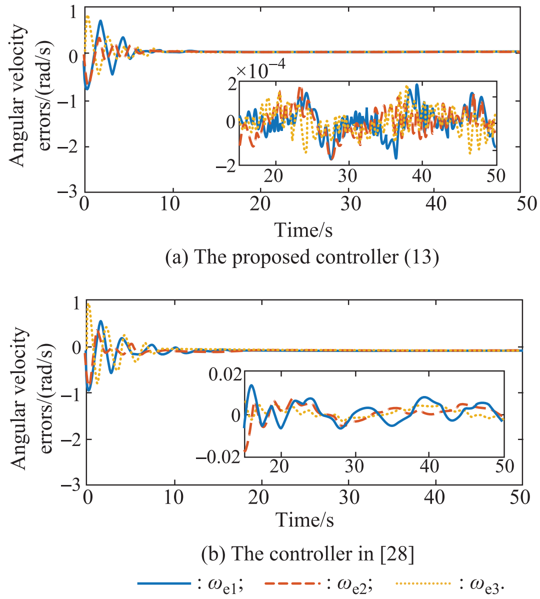

(a) The proposed controller (13)

(b) The controller in [28]

**Fig. 7 Time response of angular velocity tracking errors with disturbance**

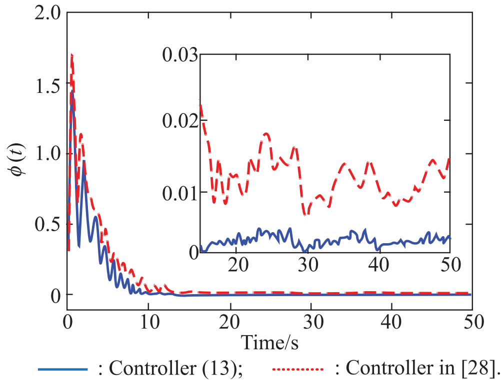


**Fig. 8 Time response of the attitude tracking errors function $\phi(t)$ with disturbance under controller (13) and controller in [28]**

Fig. 9 shows the control torques generated by (13) and that in [28] respectively. As is shown in the figure, the controller (13) outputs smaller control torques than that of the controller in [28]. Fig. 10 shows the energy consumption of the two controllers, and the amount of energy consumed by (13) is about two-thirds of that consumed by the controller in [28]. Consequently, the designed controller (13) enables the states to converge to regions containing equilibrium with faster speed, higher accuracy and less energy than that of the controller in [28] under the external disturbances.

It has been verified through the above two cases that the designed controller (13) has characteristics including high accuracy, rapid convergence speed and good robustness against disturbances. One thing should be mentioned is that the control parameters $a_5, a_6 > 0$ and $g \in (1, 2)$ can be used to set the length of the settling time, and the relationship between the time and the parameters is negatively correlated. Moreover, the parameters $a_7 > 0$ and $g \in (1, 2)$ determine the control accuracy, and the relationship between the parameters and accuracy is positively correlated. However, increasing the control parameters leads to larger control effort and fluctuation of state trajectories.

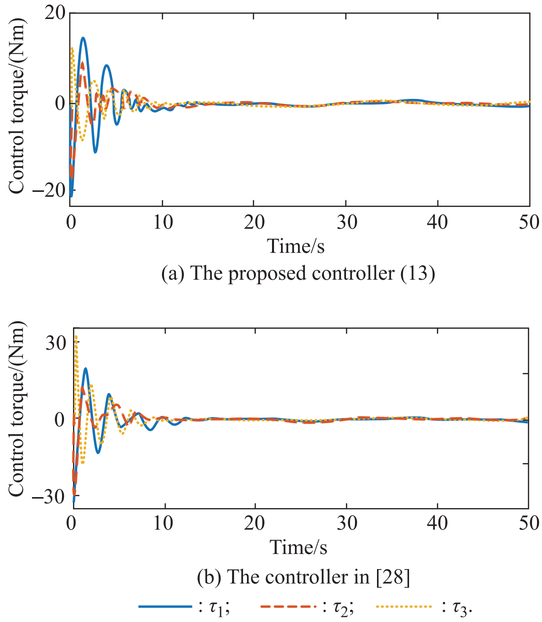


(a) The proposed controller (13)

(b) The controller in [28]

**Fig. 9 Time response of control input with disturbance**

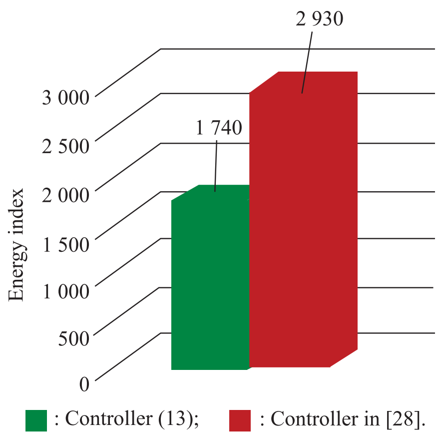


**Fig. 10 Energy index under controller (13) and controller in [28] with disturbance**

## 5. Conclusions

This study investigates the attitude tracking control for spacecraft, and proposes a finite-time output feedback attitude tracking controller without angular velocity measurements. Stability analysis shows the states can converge to a region in the presence of external disturbance. This result appears to be superior to the existing finite-time output feedback control strategy based on the homogeneous filter or observer, which cannot consider external disturbances and cannot estimate the time. Since the form of the proposed control law is simple and easy to be coded, it is expected that it can be used in the real spacecraft engineering. The results of simulations show the proposed controller can provide a good control performance.

## References

[1] W. Lu, Y. Geng, X. Chen, et al. Relative position and attitude coupled control for autonomous docking with a tumbling target. *International Journal of Control and Automation*, 2011, 4(4): 1–22.

[2] D. Jovan, Boškovic, L. Saiming, et al. Robust adaptive variable structure control of spacecraft under control input saturation. *Journal of Guidance Control & Dynamics*, 2001, 24(1): 14–22.

[3] K. Lu, Y. Xia, Z. Zhu, et al. Sliding mode attitude tracking of rigid spacecraft with disturbances. *Journal of the Franklin Institute*, 2012, 349(2): 413–440.

[4] D. Gao, J. Luo, W. Ma, et al. Nonlinear optimal control of spacecraft approaching and tracking a non-cooperative maneuvering object. *Journal of Astronautics*, 2013, 34(6): 773–781.

[5] Y. Xia, Z. Zhu, M. Fu, et al. Attitude tracking of rigid spacecraft with bounded disturbances. *IEEE Trans. on Industrial Electronics*, 2011, 58(2): 647–659

[6] I. Ali, G. Radice, J. Kim. Backstepping control design with actuator torque bound for spacecraft attitude maneuver. *Journal of Guidance, Control, and Dynamics*, 2010, 33(1): 254–259.

[7] S. Bhat, D. Bernstein. Finite-time stability of continuous autonomous systems. *SIAM Journal on Control and Optimization*, 2000, 38(3): 751–766.

[8] S. Bhat, D. Bernstein. Continuous finite-time stabilization of the translational and rotational double integrators. *IEEE Tran. on Automatic Control*, 1998, 43(5): 678–682.

[9] S. Yu, X. B. Yu. Shirinzadeh, et al. Continuous finite-time control for robotic manipulators with terminal sliding mode. *Automatica*, 2005, 40(11): 1957–1964.

[10] C. Qian, W. Lin. A continuous feedback approach to global strong stabilization of nonlinear systems. *IEEE Trans. on Automatic Control*, 2001, 46(7): 1061–1079

[11] H. Du, S. Li. Finite-time attitude stabilization for a spacecraft using homogeneous method. *Journal of Guidance, Control, and Dynamics*, 2012, 35(3): 740–748.

[12] Y. Cheng, H. Du, Y. He, et al. Distributed finite-time attitude regulation for multiple rigid spacecraft via bounded control. *Information Sciences*, 2016, 328: 144–157.

[13] S. Ding, S. Li. Stabilization of the attitude of a rigid spacecraft with external disturbances using finite-time control techniques. *Aerospace Science and Technology*, 2009, 13(4): 256–265.

[14] S. Li, S. Ding, Q. Li. Global set stabilisation of the spacecraft attitude using finite-time control technique. *International Journal of Control*, 2009, 82(5): 822–836.

[15] C. Pukdeboon. Adaptive backstepping finite-time sliding mode control of spacecraft attitude tracking. *Journal of Systems Engineering and Electronics*, 2015, 26(4): 826–839.

[16] Y. Guo, S. Song, L. Deng. Finite-time coordination control for formation flying spacecraft. *Journal of Systems Engineering and Electronics*, 2014, 25(5): 859–867.

[17] Y. Hong, J. Huang, Y. Xu. On an output feedback finite-time stabilization problem. *IEEE Trans. on Automatic Control*, 2001, 46(2): 305–309.

[18] C. Tan, X. Yu, Z. Man. Terminal sliding mode observers for a class of nonlinear systems. *Automatica*, 2010, 46(8): 1401 – 1404.

[19] C. Qian, J. Li. Global finite-time stabilization by output feedback for planar systems without observable linearization. *IEEE Trans. on Automatic Control*, 2005, 50(6): 885 – 890.

[20] H. Du, S. Li. Semi-global finite-time attitude stabilization by output feedback for a rigid spacecraft. *Proceedings of the Institution of Mechanical Engineers, Part G: Journal of Aerospace Engineering*, 2012: 0954410012464454.

[21] Q. Hu, J. Zhang. Bounded finite-time coordinated attitude control via output feedback for spacecraft formation. *Journal of Aerospace Engineering*, 2014, 28(5): 04014129.

[22] B. Xiao, Q. Hu, Y. Zhang, et al. Fault-tolerant tracking control of spacecraft with attitude-only measurement under actuator failures. *Journal of Guidance, Control, and Dynamics*, 2014, 37(3): 838 – 849.

[23] Q. Hu, B. Jiang, M. Friswell. Robust saturated finite time output feedback attitude stabilization for rigid spacecraft. *Journal of Guidance, Control, and Dynamics*, 2014, 37(6): 1914 – 1929.

[24] N. Zhou, Y. Xia, K. Lu, et al. Decentralised finite-time attitude synchronisation and tracking control for rigid spacecraft. *International Journal of Systems Science*, 2015, 46(14): 2493 – 2509.

[25] W. Cai, X. Liao, D. Song. Indirect robust adaptive fault-tolerant control for attitude tracking of spacecraft. *Journal of Guidance, Control, and Dynamics*, 2008, 31(5): 1456 – 1463.

[26] H. Du, S. Li, C. Qian. Finite-time attitude tracking control of spacecraft with application to attitude synchronization. *IEEE Trans. on Automatic Control*, 2011, 56(11): 2711 – 2717.

[27] P. Tsiotras. Further passivity results for the attitude control problem. *IEEE Trans. on Automatic Control*, 1998, 43(11): 1597 – 1600.

[28] M. Akella. Rigid body attitude tracking without angular velocity feedback. *Systems & Control Letters*, 2001, 42(4): 321 – 326.

[29] D. Thakur, S. Srikant, M. Akella. Adaptive attitude-tracking control of spacecraft with uncertain time-varying inertia parameters. *Journal of Guidance, Control, and Dynamics*, 2014, 38(1): 41 – 52.

[30] H. Gui, L. Jin, S. Xu. Simple finite-time attitude stabilization laws for rigid spacecraft with bounded inputs. *Aerospace Science and Technology*, 2015, 42: 176 – 186.

## Biographies

**Li Yuan** was born in 1974. He received his M.S. degree in guidance navigation and control from Harbin Institute of Technology in 1999. He is currently a research fellow in Beijing Institute of Control Engineering, China. He works on the technology and engineering development of spacecraft control system, and his main achievements include the guidance navigation and control (GNC) in the lunar orbiter Chang'e-1 and the soft-landing lander of Chang'e-3. He is now also a Ph.D. candidate majoring in control science and engineering, Harbin Institute of Technology, China.
E-mail: yuanli_hit@163.com

**Guangfu Ma** was born in 1963. He received his Ph.D. and M.S. degrees in electrical engineering from Harbin Institute of Technology in 1993 and 1987, respectively. In 1992, he became an associate professor and in 1997, professor at Harbin Institute of Technology, where he currently teaches and performs research in the fields of spacecraft attitude control and aerospace control systems.
E-mail: magf@hit.edu.cn

**Chuanjiang Li** was born in 1978. He received his Ph.D. degree from the Department of Control Science and Engineering, Harbin Institute of Technology in 2006. He now is a professor in the Department of Control Science and Engineering at Harbin Institute of Technology, China. His research interest convers spacecraft attitude control, optimal control and finite-time control.
E-mail: lichuan@hit.edu.cn

**Boyan Jiang** was born in 1987. He received his B.S. degree in electrical engineering and M.S. degree in navigation, guidance and control, both from Civil Aviation University of China, Tianjin, China, in 2010 and 2014, respectively. He is currently a Ph.D. candidate majoring in control science and engineering, Harbin Institute of Technology, China. His research interests include nonlinear system control, finite-time control and spacecraft attitude control.
E-mail: boyanjiang_hit@163.com